THE JOURNAL OF PHYSICAL CHEMISTRY B

Article

pubs.acs.org/JPCB

Toward in Silico Biomolecular Manipulation through Static Modes: Atomic Scale Characterization of HIV-1 Protease Flexibility

Marie Brut,*[,†,‡] Alain Estève,[†,§] Georges Landa,[†,§] and Mehdi Djafari Rouhani[†,‡]

[†]CNRS, LAAS, 7 avenue du colonel Roche, F-31400 Toulouse, France

[‡]Université de Toulouse, UPS, LAAS, F-31400 Toulouse, France

[§]Université de Toulouse, LAAS, F-31400 Toulouse, France

Supporting Information

ABSTRACT: Probing biomolecular flexibility with atomic-scale resolution is a challenging task in current computational biology for fundamental understanding and prediction of biomolecular interactions and associated functions. This paper makes use of the static mode method to study HIV-1 protease considered as a model system to investigate the full biomolecular flexibility at the atomic scale, the screening of active site biomechanical properties, the blind prediction of allosteric sites, and the design of multisite strategies to target deformations of interest. Relying on this single calculation run of static modes, we demonstrate that *in silico* predictive design of an infinite set of complex excitation fields is reachable, thanks to the storage of the static modes in a data bank that can be used to mimic single or multiatom contact and efficiently anticipate conformational changes arising from external stimuli. All along this article, we compare our results to data previously published and propose a guideline for efficient, predictive, and custom *in silico* experiments.

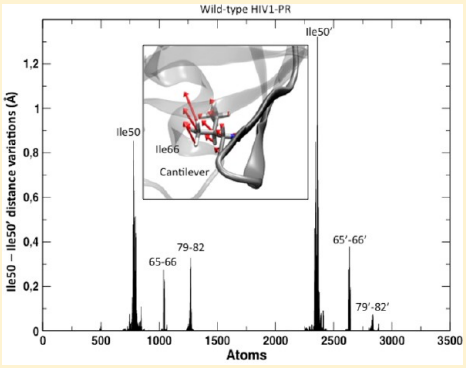

1. INTRODUCTION

Proteins are molecular machines that perform cellular functions through a complex network of intra- and intermolecular interactions. Their inherent multiscale flexibility spans from local to large structural rearrangements, allowing them to switch between different conformations. Considering the close relation existing between conformational change and protein function,[1,2] considerable experimental and theoretical efforts have been engaged in the last decades to unravel protein structures and related to interaction mechanisms. From a theoretical point of view, despite the development of numerous algorithms, understanding and predicting protein motions remains challenging, particularly for large systems.[3] Dealing with protein flexibility with an acceptable computation cost is the main difficulty, and while recent successes have been reported, flexibility degrees are just partially introduced in calculations. State of the art methods allow side chain and/or backbone flexibility, treat simplified model (articulated chain) or collective degrees of freedom, to name just a few.[4−7] Even though simplified approaches can provide useful information, predicting the structural flexibility induced by interaction at atomic level is fundamental for drug screening and biochemical function understanding at large.[8−10] This includes the understanding of the intrinsic properties of single molecules (folding), as well as interactions through the formation of macromolecular complexes (docking). Importantly, from the seminal discovery of the "induced-fit" concept, it is now well established that proteins can adapt to their partners upon interaction and have to be treated like adaptable objects.[5,9,11−14] Despite this general consensus, current modeling strategies do not fully satisfy the induced-fit concept, which is essential to understand recognition and interaction processes.[10,15,16] Recently, we proposed a new approach, called "static modes", to predict the full biomolecular flexibility at the atomic level in total adequacy with "induced-fit" requirements authorizing the blind prediction of allosteric sites, and the blind prediction of deformation response under "hand-made" design of complex external stimuli. In this view, the static mode approach is an alternative to existing normal mode based methods, which rely on natural vibrations of a molecule, here abandoned in favor of the permanent deformations caused by interactions with other molecules. More discussion on how static modes are positioned in the current methodological background can be found in our previous work references cited below.

In this article, we focus on Human Immunodeficiency Virus-1 protease (HIV-1 PR), which is a major drug target in fighting against AIDS. This enzyme is essential in the virus life cycle, by cleaving the viral polyproteins *gag* and *gag-pol* into functional proteins required for the viral infection. Using X-ray crystallography, HIV-1 PR structure was described as a C2-symmetric homodimer made up of two identical chains, each one containing 99 residues.[17,18] When HIV-1 PR is bound with a substrate, crystal structures allow identification of the active site consisting of six amino acids, characteristic of the aspartyl

Received: November 18, 2013
Revised: February 25, 2014
Published: February 25, 2014

   dx.doi.org/10.1021/jp4113156 | *J. Phys. Chem. B* 2014, 118, 2821−2830

protease family (Asp25-Thr26-Gly27 triads are found on each monomer at the dimer interface).[19−21] Thanks to experimental exploration and molecular simulation, the catalytic mechanism proposed as early as 1987[22] is now well documented.[23] Furthermore, since it plays a crucial role in the replication of HIV-1 virus, this enzyme was identified over two decades ago as a potential therapeutic target[24,25] and successfully led to the discovery of new inhibitors with a rational approach of structure-based drug design.[26−30] Recently, new generations of inhibitors bound to allosteric sites have been suggested to affect HIV-1 PR flexibility and, consequently, to disrupt its function.[31] These therapeutic strategies reinforce the importance of investigating protein flexibility to understand and possibly control the processes associated with conformational transitions. Until now, molecular dynamics[32,33] and, more recently, normal-mode analysis[9,34] have been used to relate HIV-1 PR flexibility and activity. We will show in this paper to what extent our static mode method allows these findings to be related to local solicitations of the protein, with atomistic precision.

By reason of its pharmaceutical importance, and because it presents some drug resistance due to mutations, a great amount of results relating to structure, mechanisms, or properties of HIV-1 PR were obtained by experimentation or calculation. For this reason, HIV-1 PR constitutes a good model system making it possible for us to validate the predictive nature of our method as well as to illustrate its potential beyond state of the art. In particular, we show how our static modes[35−41] can be post-treated in an interactive manner to design complex excitations. Through manipulation tools, an operator can design and evaluate an infinite set of single to multiple excitations, constraints, or interactions with no further computational cost. We have successively applied our static mode method to (i) evaluate and map molecular biomechanical properties, including blind prediction of allosteric mechanisms, in the case of HIV 1 PR; (ii) simulate and predict conformation changes induced by ligand binding; (iii) explore mutation effects; and (iv) examine multidomain excitation fields. All along this paper, we will compare our results to those already obtained with more costly methodologies and set out why our approach is particularly innovative and efficient. We will particularly address the stability of the active site through the characterization of Asp25−Asp25′ distance, as well as its accessibility enabled by the flap motion (Ile50−Asp25 distance). We will also show, with the case of M46I, how point mutations can affect this mechanism and be easily simulated to screen enzyme properties and to be further positively selected to pave the way to novel therapeutic design. We will finally demonstrate, through a preliminary example of ligand binding, how static modes can be diverted to efficiently introduce full-atom flexibility and induced-fit effects in docking strategies.

2. MATERIALS AND METHODS

HIV-1 protease was found in two conformations by X-ray crystallography: semiopen or closed, depending on its state, respectively, ligand free or bound. A fully open conformation in which the active site is accessible to substrate was not solved in crystal structures but deduced from NMR experiments. Many molecular dynamics studies have also shown that the fully open form is transient and spontaneously returns to the semiopen conformation.[29] In the first part of this study, the molecular structure of a closed protease was considered (PDB ID: 1HHP). This structure was first prepared using the AMBER11 package.[42] All hydrogen atoms were added using the LEaP program. This step is important, since the Hessian matrix used in our calculations is likely to be affected by the change of structure and atomic interactions due to different protonation states. As a consequence, the static modes will also be modified and one can imagine using this method on various protonation states to investigate the effect of pH on protein flexibility and stability. The molecule was then subjected to a total energy minimization, with an implicit solvent model and the ff99bsc0 force field.[43] This step is required to relax the structure from its crystal constraints, generate an equilibrium conformation, and extract the Hessian matrix whose elements are used to compute the static modes. Here, the use of the Hessian matrix implies that the static modes are calculated within the harmonic approximation. Anharmonic effects could be introduced using matrices of higher order. Details about the method have already been published and partial results on several biomolecules reported.[35−41] In particular, we have successfully quantitatively correlated results to experiments,[36] and probed active site stability and mutation effects on enzymatic activity.[38] The static mode method allows calculating all the deformations of a molecule submitted to elementary external excitations. Each mode contains the deformation field induced by the specific excitation of a specific molecular site. In other words, by storing this fundamental data, we can further map the molecular deformations induced by specific perturbations, explore the full flexibility of a molecule, and exploit it with a very acceptable computational cost. In this case, static mode calculation required 90 CPU minutes with a 2.8 GHz Intel Core 2 Duo processor. This corresponds to the calculation of all $3N$ static modes of a molecule containing $N = 3200$ atoms. We can point out that much larger molecules can be treated with this method with a reasonable computing time. Furthermore, in practical applications, the calculation of all static modes is not necessary. Rather, a small proportion of these modes, chosen empirically, is sufficient, reducing the computing time by the same amount. On a more general basis, the Hessian matrices of biological molecules are largely sparse, since each atom is in interaction with those in its neighborhood, of the same order of magnitude whatever the size of the molecule. The Gauss Seidel algorithm, adopted here for the calculation of static modes, is well adapted to the optimization of the computing time, since it only considers effective interactions. Therefore, for the calculation of a predefined number of static modes, the scalability of the method is of $0(N)$. In cases where all the $3N$ static modes are required, the scalability raises to $0(N^2)$. Once obtained, these modes are stored in a matrix $(3N \times 3N - 6)$ and are accessible for a post-treatment procedure to probe the "induced-fit" molecular flexibility. To this end, they are then solicited by applying single or multiple forces on the molecule and directly provide the induced deformation field. In this study, we apply forces in a systematic way to investigate the relation existing between specific residues and flexibility variations. In the following part, we first optimize the direction of the applied force in order to maximize the relevant interatomic distances that characterize active site stability and functional motions. We also expound how to use static modes to evaluate mutation effects and to perform multidomain excitation through two examples: the simulation of ligand-induced conformation change and a systematic and blind two-site perturbation.

dx.doi.org/10.1021/jp4113156 | J. Phys. Chem. B 2014, 118, 2821−2830

3. RESULTS

3.1. Force Optimization. *3.1.1. HIV-1 Protease Active Site.* Figure 1 introduces HIV-1 PR "geography" as well as the terms used in this article. We first focused on active site amino acids, especially Asp25 and Asp25′, which are directly involved in the catalytic mechanism. We particularly attempted to localize which regions can induce active site conformational changes, i.e., which amino acids impact active site stability. To this end, we systematically solicit the static modes while solving a constrained optimization problem: while conserving the amplitude of the force applied on each atom, we optimize its direction to get the maximum distance variation between two atoms. The calculation details have already been described in Brut et al.[38] For each atomic constraint, we report the resulting Cα(Asp25)−Cα(Asp25′) distance variation in Figure 2A. This graph allows localizing the residues that impact Asp25−Asp25′ distance stability and potentially enzymatic activity. We identify the following regions: two peaks with an amplitude higher than 0.5 Å correspond to Asp25/25′ residues and their neighbors (23−28 and 23′−28′). Variations around 0.05 Å are correlated with residues 83−86 and 83′−86′. Finally, with an amplitude below 0.05 Å, we find the sequences 5−11, 97−99 and their symmetric 5′−1′ and 97′−99′. These sequences respectively belong to the active site itself, the binding pockets, and the terminal domain and are, respectively, colored in red, orange, and yellow in Figure 2B for more clarity. Correlation between the active site and the binding pockets has been intensively studied with experiments[44,45] or calculation.[46−50] They notably show that mutations of residues 82−84 lead to a loss of affinity with the ligand, and that binding pocket movements are

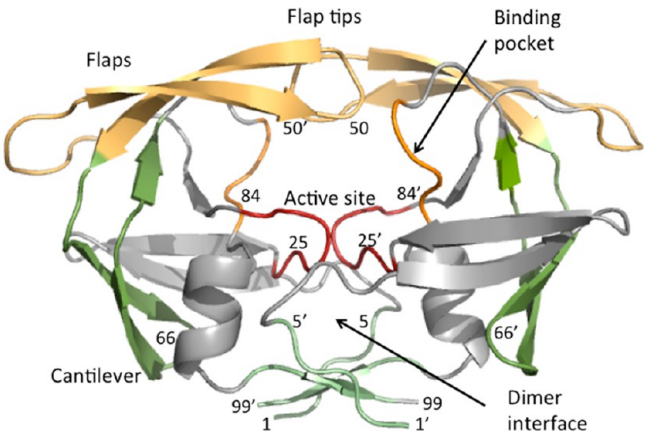

Figure 1. Three-dimensional structure of HIV-1 protease (PDB ID: 1HHP). The protein is composed of two identical monomers of 99 residues. The active site region is localized in red (residues 24−29 and 24′−29′), the flaps in yellow (residues 43−58 and 43′−58′), the binding pockets in orange (residues 81−84 and 81′−84′), the cantilever in green (residues 59−75 and 59′−75′), and the terminal region in pale green (residues 1−5/95−99 and 1′−5′/95′−99′).

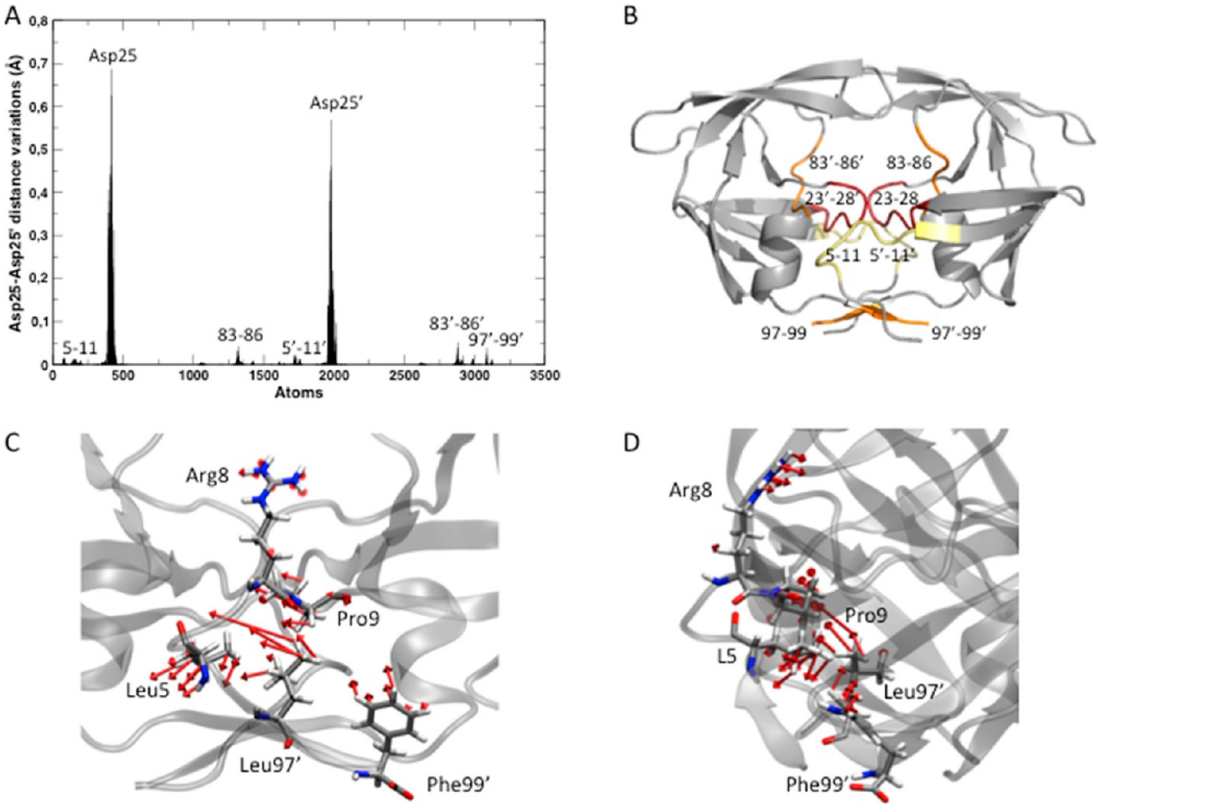

Figure 2. (A) Variations of the distance Cα(Asp25)−Cα(Asp25′) induced by the optimized excitation of each atom of the closed protease (PDB ID: 1HHP). Values are represented in angstroms. (B) The sequences correlated with the variations of Cα(Asp25)−Cα(Asp25′) distance are localized in red, orange, and yellow colors and respectively belong to the active site region, the binding pockets, and the terminal domain. Red, orange, and yellow colors correspond to deformation amplitudes larger than 0.5 Å, around 0.05 Å, and below 0.05 Å, respectively. (C) The main forces responsible for Cα(Asp25)−Cα(Asp25′) opening are represented on the interface and terminal domain (residues 5, 8−9, 97′, and 99′). Their norm is proportional to the distance variation they induce. Both front (C) and side (D) views are shown.

dx.doi.org/10.1021/jp4113156 | J. Phys. Chem. B 2014, 118, 2821−2830

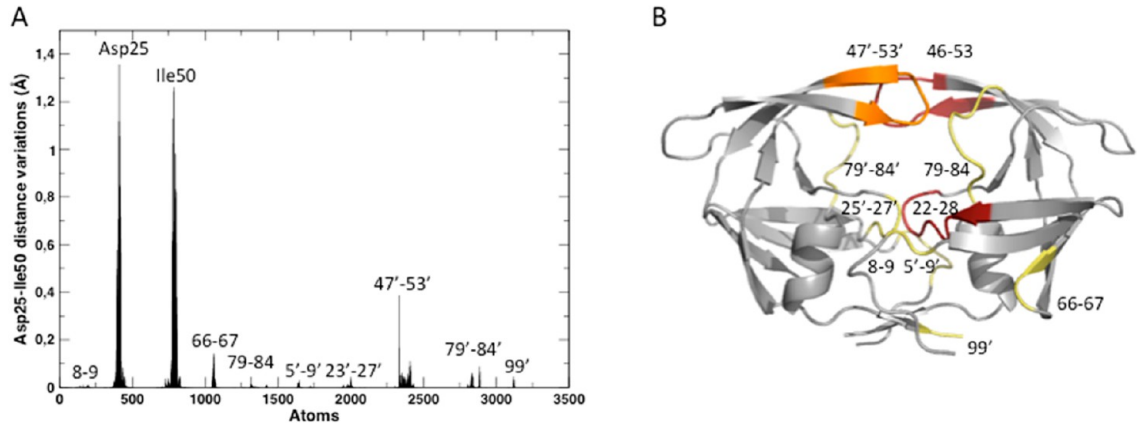

Figure 3. (A) Variations of the distance Cα(Ile50)−Cα(Asp25) induced by the optimized excitation of each atom of the closed protease (PDB ID: 1HHP) (in Å). (B) The sequences correlated with Cα(Ile50)−Cα(Asp25) distance variations are colored in red, orange, and yellow, respectively, for amplitudes larger than 0.5 Å, around 0.05 Å, and below 0.05 Å. They correspond to the active site, the flap tip region, and the cantilever regions.

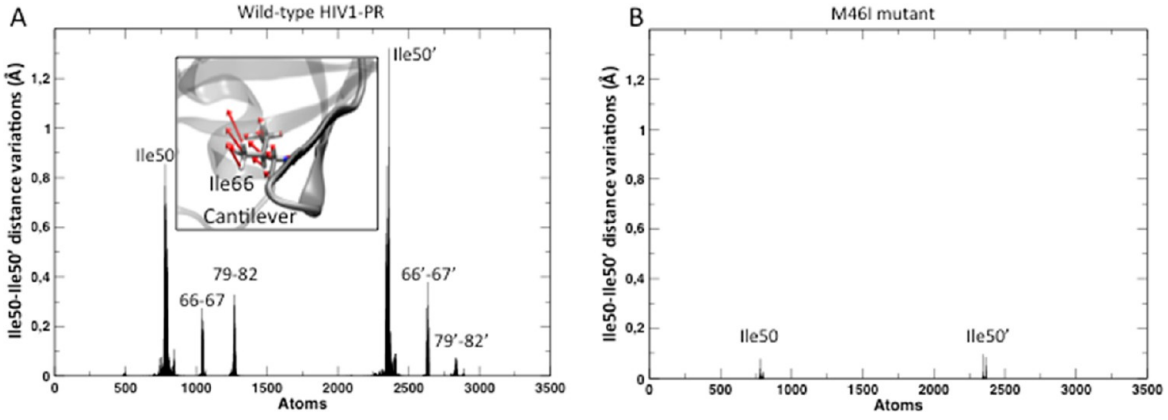

Figure 4. (A) Variations of the distance Cα(Ile50)−Cα(Ile50′) induced by the optimized excitation of each atom of the closed protease (PDB ID: 1HHP) (in Å). The directions of the forces applied on the residue Ile66 (cantilever) are also represented. (B) The same variations are represented for M46I mutant whose flexibility is drastically affected.

correlated with the ones of the active site. One of them in particular has highlighted the significant role played by G86 in maintaining the correct geometry of the HIV-1 PR active site loop, which is exactly what we show here.[51] These studies highlight the influence of dimer interface and terminal domains on the active site stability. As a matter of fact, the dimer is mainly stabilized by interactions generated between the C- and N-terminal residues of HIV-1 protease.[52−54] Modifying these interactions, by amino acid mutations or chemical modifications, for example, destabilizes the dimer, and, consequently, the active site situated at the dimer interface. This domain is currently studied as a possible therapeutic target to prevent the dimerization of HIV-1 PR.[53−55]

This simplified representation was used for the sake of clarity but does not fully assess the atomistic information contained in the static modes. We have shown until now how a single static mode run enables relevant sequences to be identified, already characterized by multiple experiments and calculations at the residue level, thus demonstrating the predictive power of our method. In the following part, we show how our approach makes it possible to explore these mechanisms with an atomistic resolution, unraveling the intimacy of each interconnected motion. Let us now focus on the terminal domain, which is currently studied as an allosteric binding site for inhibitors. As previously indicated, each distance variation shown in Figure 2A results from the application of optimized forces on each atom. Parts C and D of Figure 2 show an alternative representation of the results in Figure 2A, simplifying the visualization of atomic contributions. Here, one can find a mapping of the applied forces on each atom and the resulting Cα(Asp25)−Cα(Asp25′) distance variations. The directions of the arrows indicate the direction of the applied force, on each specific atom, which maximizes the distance variation. The lengths of the arrows are proportional to the amplitudes of the distance variations, such that longer arrows correspond to larger deformations of the active site. The longer arrows show the sites where it is easier to perturb the Cα(Asp25)−Cα(Asp25′) distance. For more clarity, only the longest arrows are shown on one side of the molecule (residues 5, 8−9, 97′, and 99′). Atomic contributions clearly involve the side chains of the residues, which highlights their role in the dimer stabilization at the interface. From Figure 2C and D, we can also identify the main contribution of the residues 5 and 9, associated with two preferential directions, one transversal to the interface plan and one directed toward the protease core.

3.1.2. Flap Opening. HIV-1 PR is found in two states: semiopen or closed, when it is, respectively, ligand-free or bound. NMR experiments and molecular dynamics have shown that both flaps covering the active site present a hinge-like motion (with an amplitude up to 7 Å).[32−34,56−60] This motion

dx.doi.org/10.1021/jp4113156 | J. Phys. Chem. B 2014, 118, 2821−2830

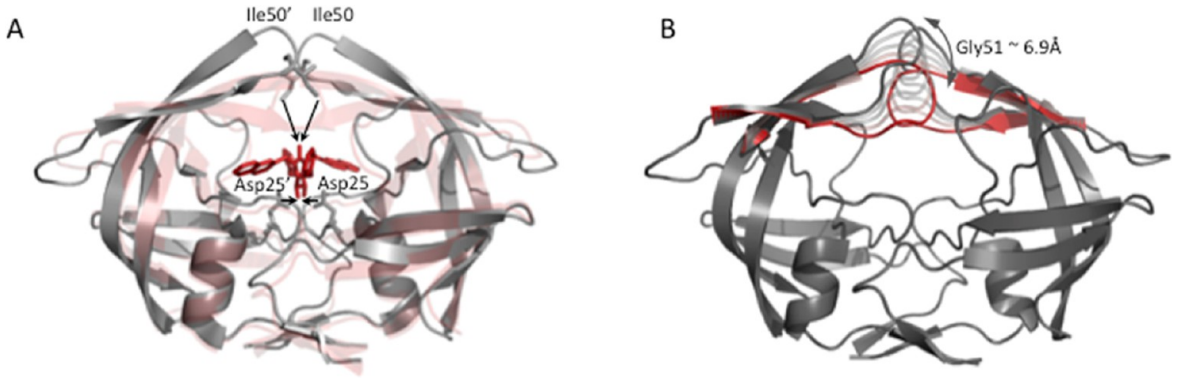

Figure 5. (A) Schematic representation of the forces applied on the Cα atoms of four residues (Asp25, Asp25′, Ile50, and Ile50′) of the open HIV-1 PR (PDB ID: 1TW7) in the direction of the oxygen atoms of a urea cyclic ligand. (B) These forces drive a flap closure evaluated by the flap tips (Ile50 and Ile50′) that cover a distance of 6.6 Å.

plays a central role in protease activity, since it controls access to the active site. To investigate which type of constraint can induce a flap motion, we considered the Asp25−Ile50 distance that separates the active site from the flap tips. The same procedure as in paragraph 3.1.1 was followed: we systematically optimized the forces applied on HIV-1 PR atoms to induce an optimum opening of the Cα(Asp25)−Cα(Ile50) distance. Optimization results are reported in Figure 3A. Both peaks with amplitudes larger than 1 Å are attributed to Asp25 and Ile50 residues and their neighbors (22−28 and 46−53, respectively), 0.4 Å peaks correspond to the second flap region, and finally lower peaks refer to sequences 25′−27′, 79−84, 79′−84′, 8−9, 5′−9′, 99′, and 66−67, respectively, situated in the active site, the binding pockets, the terminal, and cantilever regions. For sake of clarity, these residues are, respectively, represented in red, orange, and yellow in Figure 3B. We first observe that most of the sequences found in paragraph 3.1.1 also appear on this graph. Since they are correlated with Asp25 displacement, their contribution cannot be considered to conclude about the flap opening. However, the orange sequence that corresponds to the opposite flap (47′−53′) reveals a mutual drive of the flaps. Already reported in the literature,[61] this mechanism is explained by the creation of interactions between the flap tips (50−51 and 50′−51′) at the dimer interface that stabilize HIV-1 PR in its closed conformation. Mutations in this region have been shown to considerably decrease the catalytic activity. This second calculation allows also identifying a last sequence: Ile66−Cys67, i.e., the cantilever tip, whose role in relation to flap motion has been investigated, through molecular dynamics, for example.[33,46]

To corroborate these conclusions, we also optimized the forces to get an optimum opening of the Cα(Ile50)−Cα(Ile50′) distance. Results are presented in Figure 4A and again highlight the crucial role of the cantilever (66−67 and 66′−67′) in flap motions. This result is particularly interesting, since it confirms the existence of long-range communication in HIV-1 PR and is in agreement with the current strategies aiming at targeting the cantilever region.[47,48] Here again, static modes can go beyond and provide information at the atomic level. In particular, it is worth noticing that the forces applied on residue 66 (represented in Figure 4A), allowing the Cα(Ile50)−Cα(Ile50′) distance variations to be maximized, are directed upward, thus corroborating and illustrating in full detail the existence of a lever mechanism. Whereas the active role of this residue has already been reported, to our knowledge, such a level of precision in the description of the lever mechanism has not been reached.

3.1.3. Effect of Mutations on the Flap Flexibility. Many experimental and theoretical studies have reported a modification of flap flexibility correlated to point mutations in HIV-1 PR that lead to drug resistance. In particular, M46I variant is reported to be the most common compensatory mutation.[48,59,62,63] We have applied the static mode protocol to M46I mutant with the objective to evaluate its impact on flap flexibility. From the wild type HIV-1 PR structure, we substituted Met46 for Ile46 with Pymol[64] and then followed the same computational procedure as described previously. We performed a force optimization to maximize the Cα(Ile50)−Cα(Ile50′) distance. The results, shown in Figure 4B, are drastically different from those presented in Figure 4A (wild type HIV-1 PR). Only two peaks are still represented on the graph, corresponding to the residues Ile50 and Ile50′, and amplitudes are 10-fold reduced, which indicates that both systems differ in their flexibility and that HIV-1 PR is stabilized in its closed conformation. Whereas M46I mutation induces small local changes in the protein structure, it leads to considerable alteration of the flap flexibility. Previous molecular dynamics simulations have indeed indicated that this mutation favors a closed conformation relative to the wild-type protease, although the mutated protease structure is not affected compared to the wild type.[62,63,65−67] This result suggests that static modes can be safely used to predict and map alterations of flexibility in response to custom modifications like point mutations in this case.

3.2. Multidomain Excitation: Mimicking Ligand Approach. We have shown in the previous sections how static modes can be used to apply single optimized forces and to evaluate in systematic manner all atomic contributions in relation to a given induced molecular response. In this part, we follow a different procedure and apply specific forces on the active site to mimic the effect of ligand binding. We start from a semiopen conformation of HIV-1 PR, which is preferred when the enzyme is unbound: the flap tips are shifted away from the catalytic site but are still in contact with each other (PDB ID: 1TW7). We next computed the corresponding static modes and aligned a PDB structure containing a urea cyclic inhibitor (PDB ID: 1HVR) to get the relative position of the ligand in the central cavity of our structure. We then applied four forces on Ile50, Ile50′, Asp25, and Asp25′ toward the oxygen atoms of the ligand, as shown in Figure 5A, and calculated the induced

dx.doi.org/10.1021/jp4113156 | J. Phys. Chem. B 2014, 118, 2821−2830

molecular deformations (less than 1 CPU second) on Figure 5B. Applying such forces drives the flaps toward the active site, and we measured a displacement of Gly51 Cα atoms of 6.6 Å. To assess the consistency of our calculations, we also measured the backbone RMSD between our predicted structure and the experimentally solved closed form. In both cases, the flap orientation is very similar, as evidenced by the resulting RMSD of 0.30 Å down from an initial value of 1.52 Å.

We use here a very simplified model compared with the real interaction network that involves more than four residues, but this model appears to be consistent to describe the main lines of the closure mechanism.[60,61,68] From a computational point of view, we show here how static modes can be efficiently used to provide insight into protein functional motions. Beyond, this encouraging result supports our final objective of using static modes to introduce full flexibility in a docking algorithm in which the variables during the simulation process are restricted to the coordinates of constrained atoms. In this process, the docking problem can be expressed in terms of interaction sites between the two molecules, the molecular deformations being extracted from the precalculated static modes of each molecule. The molecular deformations are straightforward and driven by the evolution of intermolecular forces exerted on the interaction sites and computed at each iteration step, as the two molecules move in space. The dynamic variables during the docking process are therefore restricted to the coordinates of atoms in direct interaction. The dynamics of the remaining atoms is already contained in the static modes, which allows one to drastically simplify the procedure and save computing time. This process is particularly interesting in this, case since we show that very few forces can create flap movement. Another advantage of this approach stems from the fact that different levels of accuracy and granularity may be envisaged depending on the energy model that is used for the calculations. As we previously said, the static mode formalism neither depends on the energy nor the coordinate model. All-atom or coarse-grained representations can be equally used to introduce the degree of flexibility required in the calculations, which can be considered as a basis for further discussion on rigid domain motions and correlations.[46,47] Finally, the harmonic deformations generated thanks to the static modes can be turned into a complete conformational change by running a subsequent energy minimization.

3.3. Toward Molecular Tweezers, Another Multidomain Excitation Process. Optimizing the force direction to induce a given structural response was a first strategy to probe and localize molecular properties in a systematic way. We then showed an example of multidomain solicitation through the specificity of ligand binding. In this case, the binding site was known but we can speculate that a blind multidomain excitation would allow accessing other molecular properties, revealing pertinent correlation and activating specific mechanisms. With no a priori knowledge of molecular features, we propose to pinch every couple of atoms as the most intuitive, blind, and systematic procedure to tackle multidomain excitation.

Starting from the static modes previously calculated for the closed and open structures, we pinched every couple of atoms of HIV-1 PR with normalized forces and evaluated the response of the following distances: Cα(Asp25)−Cα(Asp25′) and Cα(Asp25)−Cα(Ile50). This step required 30 CPU minutes, given the large number $N(N-1N)/2$ of solicited couples. Results are represented in Figures 6 and 7; only the variations

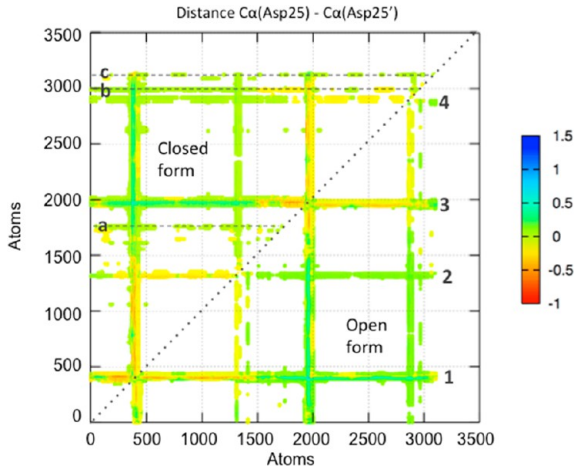

Figure 6. Variations of the distance Cα(Asp25)−Cα(Asp25′) induced by the pinching of every couple of atoms of HIV-1 PR in its closed (upper triangle, A) and open form (lower triangle, B). Variations range from −1.5 Å (in red) to 2.5 Å (in blue).

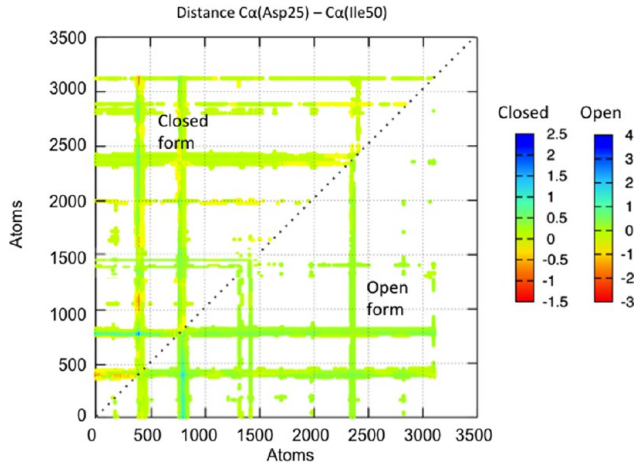

Figure 7. Variations of the distance Cα(Asp25)−Cα(Ile50) induced by the pinching of every couple of atoms of HIV-1 PR in its closed (upper triangle, A) and open form (lower triangle, B). Variations range from −0.8 Å (in red) to 1.4 Å (in blue) and from −3 Å (in red) to 4 Å (in blue) for the closed and open states, respectively.

higher than |0.1|Å are shown for better readability. We first consider the Cα(Asp25)−Cα(Asp25′) distance variations. For the closed form (see Figure 6A), variation amplitudes range from −1 to 1.5 Å. Four complete bands, numbered from 1 to 4, appear on this graph and correspond to sequences that induce a response of the active site when pinched with any other atom of the molecule. These sequences have already been found in section 3.1.1 and are already known to affect the Cα(Asp25) and Cα(Asp25′) distance: they correspond to the active site region (residues 22−27 and 22′−27′) and to the binding pockets (residues 81−84 and 81′−84′). Other preferential couples can be identified on the dotted bands a, b, and c and correspond to dimer interface sequences (respectively 7′−11′, 88′−90′, and 96′−99′) pinched with specific residues represented in Figure 8. Depending on the level of accuracy required, a deeper analysis can provide a list of these specific couples. For example, case C in Figure 8, which represents the couples that maximize Cα(Asp25) and Cα(Asp25′) distance variation and involve the α-helix of the terminal domain

dx.doi.org/10.1021/jp4113156 | J. Phys. Chem. B 2014, 118, 2821−2830

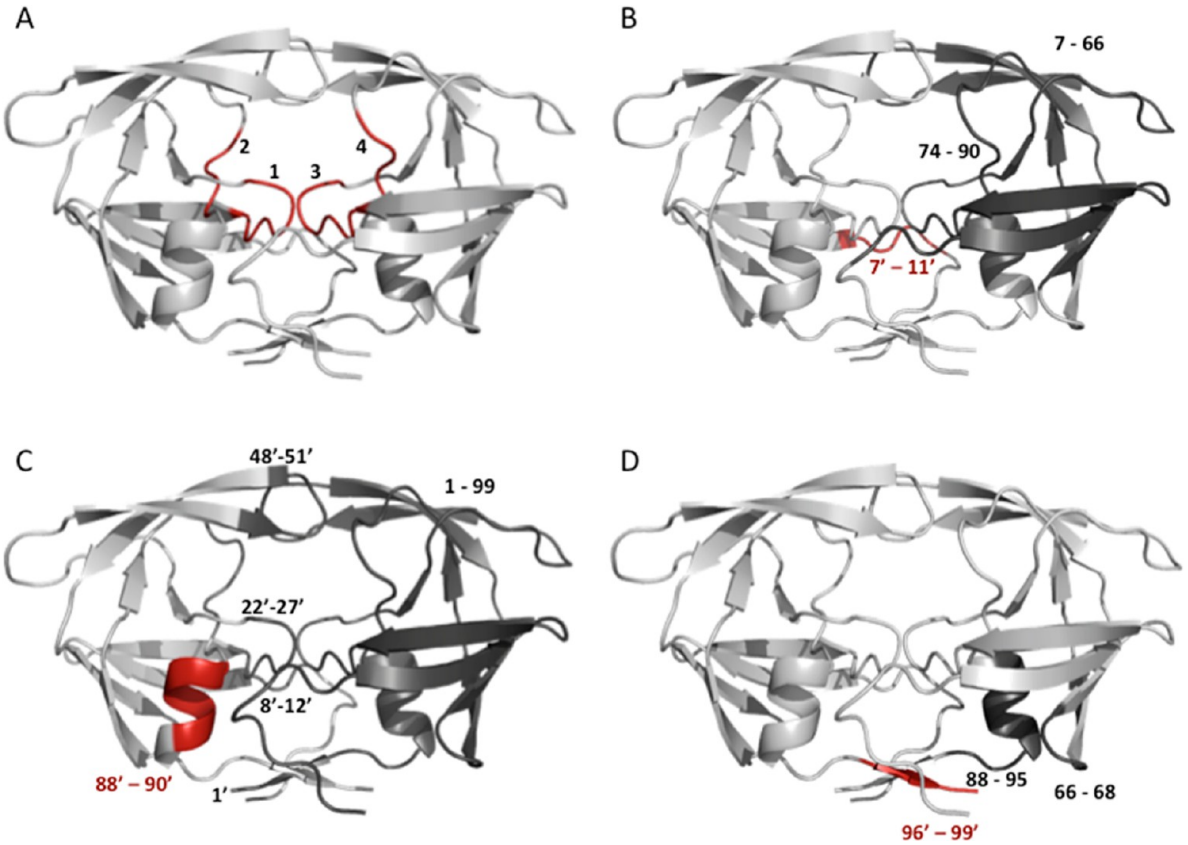

Figure 8. The sequences 1−4 of Figure 6A, whose atoms induce a variation of the distance Cα(Asp25)−Cα(Asp25′) when pinched with any other atom of the molecule, are shown in part A. The sequences corresponding to the dotted lines a, b, and c are represented in red on the molecules B, C, and D, respectively. In each case, red sequences correspond to interface residues (in red: respectively 107−111, 188−190, and 195−198) that require being pinched together with dark red residues to generate a variation of the distance Cα(Asp25)−Cα(Asp25′).

(residues 88−91,) implies Leu90′ methyl groups and Lys14′ side chain amino group.

Figure 7A presents the same calculation run for Cα(Asp25)−Cα(Ile50) distance variations. The resulting values range from −1.5 to 2.5 Å. Again, only the variations higher than |0.1|Å are shown for the sake of clarity. Four bands numbered from 1 to 4 let four sequences be identified whose pinch with any other residue induces a flap motion. Again, they correspond to the sequences previously found in section 3.1.1: the active site region (22−27), the flap tips (47−53 and 47′−53′), and a C-terminal tip (97′−99′). Eight new specific regions, noted a−h, are identified here, and involve some dimer interface sequences and the cantilevers (see Figure S1, Supporting Information). In this case, multiple excitations do not bring new information compared to single excitation. However, this new "cartography" may help to find a new way to act on the protein activity, in particular for the design of a multidomain inhibitor.

Finally, in order to evaluate any possible differences between the behaviors of the semiopen and closed forms upon pinching, the same procedure was applied to the semiopen protease. The results obtained for Cα(Asp25)−Cα(Asp25′) and Cα-(Asp25)−Cα(Ile50) distances are presented in Figures 6 and 7, respectively. In Figure 6B, while amplitudes are similar to those found in the closed form (ranging from −1 to 1.5 Å), several differences clearly appear when considering the atom contribution. Bands 1−4 do not present any significant change, but the dimer interface sequences (dotted lines a, b, and c in the closed form) are no more active. Interestingly, previous studies (NMR experiments, for example[57]) have experienced a loss a flexibility of interface chains in the free protease compared with the bound one. Our interpretation is that the mobility of interface chains probably allows an easier accommodation of the active site, not required in the free semiopen protease. Figure 7B shows the variations of Cα(Asp25)−Cα(Ile50) distance on the semiopen form (on the right) and appears to differ drastically from the closed form (on the left). Importantly, amplitudes are larger, ranging from −3 to 4 Å, compared to −1.5 to 2.5 Å in the closed form, pointing to the flexibility increase of the semiopen form of HIV-1 PR. Many weak bonds between the flaps, and between the flaps and the active site, exist in the closed form but are broken in the semiopen form, allowing a larger flap motion. In addition, the upper right quarter of the graph, corresponding to intramonomer pinches of 1′−99′ monomer, has nearly disappeared. This observation suggests a loss of affinity at the dimer interface and, consequently, a loss of correlation between both monomers.

Several papers have recently reported how molecular clips and tweezers can bind multiple sites of an enzyme and induce new synergetic effects.[69−72] The first developed molecules exploit multiple aromatic interactions and selectively target proteins with specific amino acid residues. Potential applications are expected for drug delivery, in particular. The last calculations presented in this article are particularly well suited to these new drug strategies targeting multiple molecular sites.

dx.doi.org/10.1021/jp4113156 | J. Phys. Chem. B 2014, 118, 2821−2830

4. DISCUSSION AND CONCLUSION

In this paper, we demonstrate that our static mode approach, after being presented and exposed on various molecular targets,[35,36,38−41] enables concentrating all the information required for studying biomechanical properties at large within a costless framework in terms of calculation time and an infinite capability of considering biomolecular excitation. Through this study, thanks to the static mode method, we have rapidly collected many essential properties of a model system, namely, HIV-1 PR, properties already derived from multiple experimental or computational methods during the last 20 years. Such a compilation is the result of a 1.5 h calculation of the static modes, plus 30 min of post treatment, illustrating the efficiency and the predictive capacity of the method. In this paper, we particularly focused on the screening of active site biomechanical properties, the blind prediction of allosteric sites, and the design of multisite strategies to target deformations of interest. Along with the points above investigated to validate our approach, we demonstrated that the atomistic mechanisms can be understood with a high level of accuracy. This makes it possible to depict which atom and pertinent excitation can induce a given deformation field. We particularly validated our predictions on (i) the role of binding pockets in active site stability,[31,44−46,49] (ii) the influence of the interface domain (particularly C-terminal domain) on active site stability,[28,46,49] (iii) the cantilever mechanism inducing flap motion,[46,48] (iv) the existence and cartography of rigid domains,[49,73] (v) the different mechanical behavior between closed/semiopen protein (notably concerning the role of dimer interface on monomer communication, flap flexibility, and global dimer stability),[57] (vi) the simulation of flap closure induced by a ligand,[56,68,74] (vii) the effect of M46I mutation on flap flexibility.[59,63]

These results and their agreement with the great number of quoted data authorize us to evaluate the relevance of the static mode method for the exploration of protein biomechanical properties. Since all information about possible molecular deformation and internal correlation is encoded in the static modes, they appear as a strategic and original tool to mimic single or multiatom contact, and to efficiently anticipate conformational changes arising from external stimuli. However, several questions remain to discuss if one envisages to use the static modes to efficiently perform conformational changes. Notably, although nonharmonic terms are at the origin of multiple configurations generally observed in biomolecules, they have not been taken into account in our calculations so far. Anharmonicity is most of all related to side chain motions of low energy. To the extent that the anharmonic contribution can be considered as an energy perturbation, the static mode formalism allows one to account for this contribution by using matrices of higher order that the Hessian matrix. One should then consider a longer computing time but also a significant increase in storage capacity. A second question stems from the impact of the starting conformation on the static mode results. One can ask if similar effects may be observed starting with various close configurations or if conformational change can be performed using the static modes of a single starting configuration. With the atomic displacements in different static modes being determined via the inversion of the Hessian matrix, they are mainly governed by the largest force constants. These elements correspond to the most rigid parts of the molecule and are not expected to undergo large changes in configurations. As long as these elements are not seriously modified, the approach can be considered as robust. However, for the same reason, a single static mode calculation cannot lead to conformational change, since it is valid for small deviations from the starting structure. Conformational change can be performed exploring the pathway built through a succession of deformation/relaxation steps, in which static modes will be recalculated when necessary. A similar strategy was proposed and discussed in a previous work to investigate the conformational changes of the amyloid $\beta(1-16)$ peptide induced by Zn^{2+} ions.[41]

From a technical point of view, we propose here a guideline for efficient, predictive, and custom *in silico* experiments, showing how external forces enable the virtual manipulation of a molecule. Through the widely investigated case of HIV-1 protease, we have presented several practical applications of the static modes used to probe the intrinsic flexibility of a molecule, to understand its activity and to propose customized strategies to modify it.

Beyond these conclusions, our results on the prediction of ligand-induced deformation allow us to consider the use of static modes to implement full-atom flexibility in the future and more complex multilevel strategies, notably for interaction processes or screening procedures, which is a mainstream focus of current methodological developments. Our future goal is to make accessible a static mode data bank to authorize any user to run its own in silico experiments (HIV-1 PR static modes are already available from our web page[75]). We believe that our modeling approach brings new perspectives to improve the understanding of biomolecular processes. It can be advantageously used as a predictive tool to guide experiments, at least qualitatively. The virtual experiments that we propose would be helpful as a first step to propose new therapeutic strategies but also to design custom functions for biohybrid technologies where biomolecules are expected to play a key role.

■ ASSOCIATED CONTENT

Ⓢ Supporting Information

Sequence details of the atomic contributions presented in Figure 7A are given in Figures S1 and S2. This material is available free of charge via the Internet at http://pubs.acs.org.

■ AUTHOR INFORMATION

Corresponding Author

*E-mail: mbrut@laas.fr. Phone: 00(33)561336304.

Notes

The authors declare no competing financial interest.

■ ACKNOWLEDGMENTS

This work was supported by the French National Agency for Research (ANR-VIBBnano) and the European COST project (Biointegrated technologies). We thank the CALMIP Supercomputer Center for CPU resources.

■ REFERENCES

(1) Teilum, K.; Olsen, J. G.; Kragelund, B. B. Functional Aspects of Protein Flexibility. *Cell. Mol. Life Sci.* **2009**, *66*, 2231−2247.

(2) Teilum, K.; Olsen, J. G.; Kragelund, B. B. Protein Stability, Flexibility and Function. *Biochim. Biophys. Acta* **2010**, *1814*, 969−976.

(3) Zhang, Y. Progress and Challenges in Protein Structure Prediction. *Curr. Opin. Struct. Biol.* **2008**, *18*, 342−348.

(4) Schlick, T.; Collepardo-Guevara, R.; Halvorsen, L. A.; Jung, S.; Xiao, X. Biomolecular Modeling and Simulation: a Field Coming of Age. *Q. Rev. Biophys.* **2011**, *44*, 191−228.
(5) Skjaerven, L.; Reuter, N.; Martinez, A. Dynamics, Flexibility and Ligand-Induced Conformational Changes in Biological Macromolecules: a Computational Approach. *Future Med. Chem.* **2011**, *3*, 2079−2100.
(6) van Gunsteren, W. F.; Bakowies, D.; Baron, R.; Chandrasekhar, I.; Christen, M.; Daura, X.; Gee, P.; Geerke, D. P.; Glattli, A.; Hunenberger, P. H.; et al. Biomolecular Modeling: Goals, Problems, Perspectives. *Angew. Chem., Int. Ed. Engl.* **2006**, *45*, 4064−4092.
(7) van Gunsteren, W. F.; Dolenc, J. Biomolecular Simulation: Historical Picture and Future Perspectives. *Biochem. Soc. Trans.* **2008**, *36*, 11−15.
(8) Zhang, Y. Protein structure prediction: when is it useful? *Curr. Opin. Struct. Biol.* **2009**, *19*, 145−155.
(9) Boehr, D. D.; Nussinov, R.; Wright, P. E. The Role of Dynamic Conformational Ensembles in Biomolecular Recognition. *Nat. Chem. Biol.* **2009**, *5*, 789−796.
(10) Tuffery, P.; Derreumaux, P. Flexibility and Binding Affinity in Protein−Ligand, Protein−Protein and Multi-Component Protein Interactions: Limitations of Current Computational Approaches. *J. R. Soc., Interface* **2012**, *9*, 20−33.
(11) Csermely, P.; Palotai, R.; Nussinov, R. Induced Fit, Conformational Selection and Independent Dynamic Segments: an Extended View of Binding Events. *Trends Biochem. Sci.* **2010**, *35*, 539−546.
(12) Janin, J.; Sternberg, M. J. Protein Flexibility, Not Disorder, is Intrinsic to Molecular Recognition. *F1000 Biol. Rep.* **2013**, *5*, 2.
(13) Karplus, M. Dynamical Aspects of Molecular Recognition. *J. Mol. Recognit.* **2010**, *23*, 102−104.
(14) Okazaki, K.; Takada, S. Dynamic Energy Landscape View of Coupled Binding and Protein Conformational Change: Induced-Fit versus Population-Shift Mechanisms. *Proc. Natl. Acad. Sci. U.S.A.* **2008**, *105*, 11182−11187.
(15) Carlson, H. A. Protein Flexibility and Drug Design: How to Hit a Moving Target. *Curr. Opin. Chem. Biol.* **2002**, *6*, 447−452.
(16) Teague, S. J. Implications of protein flexibility for drug discovery. *Nat. Rev. Drug Discovery* **2003**, *2*, 527−541.
(17) Navia, M. A.; Fitzgerald, P. M. D.; McKeever, B. M.; Leu, C.-T.; Heimbach, J. C.; Herber, W. K.; Sigal, I. S.; Darke, P. L.; Springer, J. P. Three-Dimensional Structure of Aspartyl Protease from Human Immunodeficiency Virus HIV-1. *Nature* **1989**, *337*, 615−620.
(18) Vondrasek, J.; Wlodawer, A. HIVdb: A Database of the Structures of Human Immunodeficiency Virus Protease. *Proteins* **2002**, *49*, 429−431.
(19) Wlodawer, A.; Miller, M.; Schneider, J.; Sathyanarayana, B. K.; Toth, M. V.; Marshall, G. R.; Clawson, L.; Selk, L.; Kent, S. B. Conserved Folding in Retroviral Proteases: Crystal Structure of a Synthetic HIV-1 Protease. *Science* **1989**, *246*, 1149−1152.
(20) Mager, P. P. The Active Site of HIV-1 Protease. *Med. Res. Rev.* **2001**, *21*, 348−353.
(21) Davies, D. R. The Structure and Function of the Aspartic Proteinases. *Annu. Rev. Biophys. Biophys. Chem.* **1990**, *19*, 189−215.
(22) Suguna, K.; Padlan, E. A.; Smith, C. W.; Carlson, W. D.; Davies, D. R. Binding of a Reduced Peptide Inhibitor to the Aspartic Proteinase from Rhizopus Chinensis: Implications for a Mechanism of Action. *Proc. Natl. Acad. Sci. U.S.A.* **1987**, *84*, 7009−7013.
(23) Brik, A.; Wong, C. H. HIV-1 Protease: Mechanism and Drug Discovery. *Org. Biomol. Chem.* **2003**, *1*, 5−14.
(24) Huff, J. R. HIV Protease: a Novel Chemotherapeutic Target for AIDS. *J. Med. Chem.* **1991**, *34*, 2305−2314.
(25) Wensing, A. M.; van Maarseveen, N. M.; Nijhuis, M. Fifteen Years of HIV Protease Inhibitors: Raising the Barrier to Resistance. *Antiviral Res.* **2010**, *85*, 59−74.
(26) Wlodawer, A.; Vondrasek, J. Inhibitors of HIV-1 Protease: A Major Success of Structure-Assisted Drug Design. *Annu. Rev. Biophys. Biomol. Struct.* **1998**, *27*, 249−284.
(27) Volarath, P.; Harrison, R. W.; Weber, I. T. Structure Based Drug Design for HIV Protease: From Molecular Modeling to Cheminformatics. *Curr. Top. Med. Chem.* **2007**, *7*, 1030−1038.
(28) Lebon, F.; Ledecq, M. Approaches to the Cesign of Effective HIV-1 Protease Inhibitors. *Curr. Med. Chem.* **2010**, *7*, 455−477.
(29) Hornak, V.; Simmerling, C. Targeting Structural Flexibility in HIV-1 Protease Inhibitor Binding. *Drug Discovery Today* **2007**, *12*, 132−138.
(30) Chang, M. W.; Ayeni, C.; Breuer, S.; Torbett, B. E. Virtual Screening for HIV Protease Inhibitors: a Comparison of AutoDock 4 and Vina. *PLoS One* **2010**, *5*, e11955.
(31) Perryman, A. L.; Zhang, Q.; Soutter, H. H.; Rosenfeld, R.; McRee, D. E.; Olson, A. J.; Elder, J. E.; Stout, C. D. Fragment-Based Screen against HIV Protease. *Chem. Biol. Drug Des.* **2010**, *75*, 257−268.
(32) Karthik, S.; Senapati, S. Dynamic Flaps in HIV-1 Protease Adopt Unique Ordering at Different Stages in the Catalytic Cycle. *Proteins* **2011**, *79*, 1830−1840.
(33) Sadiq, S. K.; De Fabritiis, G. Explicit Solvent Dynamics and Energetics of HIV-1 Protease Flap Opening and Closing. *Proteins* **2010**, *78*, 2873−2885.
(34) Batista, P.; Pandey, G.; Pascutti, P.; Bisch, P.; Perahia, D.; Robert, C. Free Energy Profiles along Consensus Normal Modes Provide Insight into HIV-1 Protease Flap Opening. *J. Chem. Theory Comput.* **2011**, *7*, 2348−2352.
(35) Brut, M.; Estève, A.; Landa, G.; Djafari Rouhani, M. Mimicking DNA Stretching with the Static Mode Method: Shear Stress versus Transverse Pulling Stress. *Eur. Phys. J. E* **2012**, *35*, 75−83.
(36) Brut, M.; Estève, A.; Landa, G.; Dkhissi, A.; Renvez, G.; Djafari Rouhani, M.; Gauchard, D. Atomic-Scale Determination of DNA Conformational Response to Strained Furanose: a Static Mode Approach. *Tetrahedron* **2010**, *66*, 9123−9128.
(37) Brut, M.; Estève, A.; Landa, G.; Renvez, G.; Djafari Rouhani, M. The Static Modes: an Alternative Approach for the Treatment of Macro- and Bio-Molecular Induced-Fit Flexibility. *Eur. Phys. J. E* **2009**, *28*, 17−25.
(38) Brut, M.; Estève, A.; Landa, G.; Renvez, G.; Djafari Rouhani, M.; Vaisset, M. Atomic Scale Determination of Enzyme Flexibility and Active Site Stability through Static Modes: Case of Dihydrofolate Reductase. *J. Phys. Chem. B* **2011**, *115*, 1616−1622.
(39) Brut, M.; Estève, A.; Landa, G.; Renvez, G.; Djafari Rouhani, M.; Vaisset, M.; Gauchard, D. Deformation of Thiolated Nucleic Acid Deposited on a Silicon Surface: A Static Mode Approach. *Mater. Sci. Eng., B* **2010**, *169*, 23−27.
(40) Brut, M.; Trapaidze, A.; Estève, A.; Bancaud, A.; Estève, D.; Landa, G.; Djafari Rouhani, M. Bringing Aptamers into Technologies: Impact of Spacer Terminations. *Appl. Phys. Lett.* **2012**, *100*, 163702.
(41) Renvez, G.; Estève, A.; Landa, G.; Brut, M.; Djafari Rouhani, M.; Dkhissi, A. The Electrostatic Probe: a Tool for the Investigation of the Aβ(1−16) Peptide Deformations Using the Static Modes. *Phys. Chem. Chem. Phys.* **2011**, *13*, 14611−14616.
(42) Case, D.; Darden, T.; Cheatham, T.; Simmerling, C.; Wang, J.; Duke, R.; Luo, R.; Walker, R.; Zhang, W.; Merz, K.; et al. *AMBER 11*; University of San Francisco: San Francisco, CA, 2010.
(43) Perez, A.; Marchan, I.; Svozil, D.; Sponer, J.; Cheatham, T. E., 3rd; Laughton, C. A.; Orozco, M. Refinement of the AMBER Force Field for Nucleic Acids: Improving the Description of α/γ Conformers. *Biophys. J.* **2007**, *92*, 3817−3829.
(44) Short, G. F., 3rd; Laikhter, A. L.; Lodder, M.; Shayo, Y.; Arslan, T.; Hecht, S. M. Probing the S1/S1‘ Substrate Binding Pocket Geometry of HIV-1 Protease with Modified Aspartic Acid Analogues. *Biochemistry* **2000**, *39*, 8768−8781.
(45) Muzammil, S.; Ross, P.; Freire, E. A Major Role for a Set of Non-Active Site Mutations in the Development of HIV-1 Protease Drug Resistance. *Biochemistry* **2003**, *42*, 631−638.
(46) Harte, W. E., Jr.; Swaminathan, S.; Mansuri, M. M.; Martin, J. C.; Rosenberg, I. E.; Beveridge, D. L. Domain Communication in the Dynamical Structure of Human Immunodeficiency Virus 1 Protease. *Proc. Natl. Acad. Sci. U.S.A.* **1990**, *87*, 8864−8868.

(47) Perryman, A. L.; Lin, J. H.; McCammon, J. A. Restrained Molecular Dynamics Simulations of HIV-1 Protease: the First Step in Validating a New Target for Drug Design. *Biopolymers* **2006**, *82*, 272−284.
(48) Perryman, A. L.; Lin, J. H.; McCammon, J. A. Optimization and Computational Evaluation of a Series of Potential Active Site Inhibitors of the V82F/I84V Drug-resistant Mutant of HIV-1 Protease: an Application of the Relaxed Complex Method of Structure-based Drug Design. *Protein Sci.* **2004**, *13*, 1108−1123.
(49) Rose, R. B.; Craik, C. S.; Stroud, R. M. Domain Flexibility in Retroviral Proteases: Structural Implications for Drug Resistant Mutations. *Biochemistry* **1998**, *37*, 2607−2621.
(50) Braz, A. S.; Tufanetto, P.; Perahia, D.; Scott, L. P. Relation Between Flexibility and Positively Selected HIV-1 Protease Mutants Against Inhibitors. *Proteins* **2012**, *80*, 2680−2691.
(51) Ishima, R.; Gong, Q.; Tie, Y.; Weber, I. T.; Louis, J. M. Highly Conserved Glycine 86 and Arginine 87 Residues Contribute Differently to the Structure and Activity of the Mature HIV-1 Protease. *Proteins* **2010**, *78*, 1015−1025.
(52) Levy, Y.; Caflisch, A.; Onuchic, J. N.; Wolynes, P. G. The Folding and Dimerization of HIV-1 Protease: Evidence for a Stable Monomer from Simulations. *J. Mol. Biol.* **2004**, *340*, 67−79.
(53) Babe, L. M.; Rose, J.; Craik, C. S. Synthetic "Interface" Peptides Alter Dimeric Assembly of the HIV 1 and 2 Proteases. *Protein Sci.* **1992**, *1*, 1244−1253.
(54) Agniswamy, J.; Sayer, J. M.; Weber, I. T.; Louis, J. M. Terminal Interface Conformations Modulate Dimer Stability Prior to Amino Terminal Autoprocessing of HIV-1 Protease. *Biochemistry* **2012**, *51*, 1041−1050.
(55) Koh, Y.; Matsumi, S.; Das, D.; Amano, M.; Davis, D. A.; Li, J.; Leschenko, S.; Baldridge, A.; Shioda, T.; Yarchoan, R.; et al. Potent Inhibition of HIV-1 Replication by Novel Non-peptidyl Small Molecule Inhibitors of Protease Dimerization. *J. Biol. Chem.* **2007**, *282*, 28709−28720.
(56) Hornak, V.; Okur, A.; Rizzo, R. C.; Simmerling, C. HIV-1 Protease Flaps Spontaneously Close to the Correct Structure in Simulations Following Manual Placement of an Inhibitor into the Open State. *J. Am. Chem. Soc.* **2006**, *128*, 2812−2813.
(57) Ishima, R.; Freedberg, D. I.; Wang, Y. X.; Louis, J. M.; Torchia, D. A. Flap Opening and Dimer-Interface Flexibility in the Free and Inhibitor-Bound HIV Protease, and their Implications for Function. *Structure* **1999**, *7*, 1047−1055.
(58) Ishima, R.; Louis, J. M. A Diverse View of Protein Dynamics from NMR Studies of HIV-1 Protease Flaps. *Proteins* **2008**, *70*, 1408−1415.
(59) Lauria, A.; Ippolito, M.; Almerico, A. M. Molecular Dynamics Studies on HIV-1 Protease: a Comparison of the Flap Motions between Wild Type Protease and the M46I/G51D Double Mutant. *J. Mol. Model.* **2007**, *13*, 1151−1156.
(60) Toth, G.; Borics, A. Closing of the Flaps of HIV-1 Protease Induced by Substrate Binding: A Model of a Flap Closing Mechanism in Retroviral Aspartic Proteases. *Biochemistry* **2006**, *45*, 6606−6614.
(61) Nicholson, L. K.; Yamazaki, T.; Torchia, D. A.; Grzesiek, S.; Bax, A.; Stahl, S. J.; Kaufman, J. D.; Wingfield, P. T.; Lam, P. Y. S.; Jadhav, P. K.; et al. Flexibility and Function in HIV-1 Protease. *Nat. Struct. Biol.* **1995**, *2*, 274−280.
(62) Piana, S.; Carloni, P.; Parrinello, M. Role of Conformational Fluctuations in the Enzymatic Reaction of HIV-1 Protease. *J. Mol. Biol.* **2002**, *319*, 567−583.
(63) Piana, S.; Carloni, P.; Rothlisberger, U. Drug Resistance in HIV-1 Protease: Flexibility-Assisted Mechanism of Compensatory Mutations. *Protein Sci.* **2002**, *11*, 2393−2402.
(64) *The PyMOL Molecular Graphics System*, version 1.5.0.4; Schrödinger, LLC.: New York, 2010.
(65) Collins, J. R.; Burt, S. K.; Erickson, J. W. Flap Opening in HIV-1 Protease Simulated by 'Activated' Molecular Dynamics. *Nat. Struct. Biol.* **1995**, *2*, 334−338.
(66) Li, D.; Ji, B.; Hwang, K.; Huang, Y. Crucial Roles of the Subnanosecond Local Dynamics of the Flap Tips in the Global Conformational Changes of HIV-1 Protease. *J. Phys. Chem. B* **2010**, *114*, 3060−3069.
(67) Markowitz, M.; Mo, H.; Kempf, D. J.; Norbeck, D. W.; Bhat, T. N.; Erickson, J. W.; Ho, D. D. Selection and Analysis of Human Immunodeficiency Virus Type 1 Variants with Increased Resistance to ABT-538, a Novel Protease Inhibitor. *J. Virol.* **1995**, *69*, 701−706.
(68) Jagodzinski, F.; Brock, O. *Towards a Mechanistic View of Protein Motion*, 46th IEEE Conference on Decision and Control, 2007; 4557−4562.
(69) Jiang, Q. Q.; Bartsch, L.; Sicking, W.; Wich, P. R.; Heider, D.; Hoffmann, D.; Schmuck, C. A New Approach to Inhibit Human β-Tryptase by Protein Surface Binding of Four-Armed Peptide Ligands with Two Different Sets of Arms. *Org. Biomol. Chem.* **2013**, *11*, 1631−1639.
(70) Klarner, F. G.; Schrader, T. Aromatic Interactions by Molecular Tweezers and Clips in Chemical and Biological Systems. *Acc. Chem. Res.* **2013**, *46*, 967−978.
(71) Talbiersky, P.; Bastkowski, F.; Klarner, F. G.; Schrader, T. Molecular Clip and Tweezer Introduce New Mechanisms of Enzyme Inhibition. *J. Am. Chem. Soc.* **2008**, *130*, 9824−9828.
(72) Kessler, J.; Jakubek, M.; Dolensky, B.; Bour, P. Binding Energies of Five Molecular Pincers Calculated by Explicit and Implicit Solvent Models. *J. Comput. Chem.* **2012**, *33*, 2310−2317.
(73) Kumar, M.; Hosur, M. V. Adaptability and Flexibility of HIV-1 Protease. *Eur. J. Biochem.* **2013**, *270*, 1231−1239.
(74) Lam, P. Y.; Jadhav, P. K.; Eyermann, C. J.; Hodge, C. N.; Ru, Y.; Bacheler, L. T.; Meek, J. L.; Otto, M. J.; Rayner, M. M.; Wong, Y. N. Rational Design of Potent, Bioavailable, Nonpeptide Cyclic Ureas as HIV Protease Inhibitors. *Science* **1994**, *263*, 380−384.
(75) http://www.laas.fr/N2IS-EN/28-32287-FleXible-a-tool-for-flexible-accommodation-of-biomolecules.php.